A Fluorescence Assay for Leucine Zipper Dimerization: Avoiding Unintended Consequences of Fluorophore Attachment

David L. Daugherty and Samuel H. Gellman*

Contribution from the Department of Chemistry, University of Wisconsin, Madison, Wisconsin 53706

Received January 19, 1999

Abstract: Formation of α-helical coiled-coil dimers represents one of the simplest examples of a specific protein−protein interaction. This dimerization mode is commonly observed among transcription regulator proteins, where the process is referred to as leucine zipper formation. Inhibitors of leucine zipper dimerization would allow one to control gene expression. As a first step toward identifying such inhibitors, we have developed a fluorescence-based assay for homodimerization of peptides corresponding to the leucine zipper region of the Jun protein. The assay involves attachment of 7-hydroxycoumarin to the N-terminus of the Jun peptide. Upon dimerization, pairs of fluorophores are held near one another, which leads to self-quenching. Disruption of the dimer is signaled by an increase of 7-hydroxycoumarin fluorescence. Development of this assay proved to be more complex than expected, because we found that two commonly used fluorescent tags, pyrene and fluorescein, induce high-order aggregation of leucine zipper−fluorophore conjugates. This aggregation was demonstrated to result from cooperativity between the fluorophore and peptide portions. A third common fluorophore, 7-diethylaminocoumarin, significantly stabilized the Jun homodimer. Of the four fluorophores we examined, 7-hydroxycoumarin caused the least perturbation of leucine zipper peptide behavior.

Introduction

Protein−protein recognition underlies a wide array of physiological processes,[1] and there is considerable interest in agents that block specific protein−protein interactions.[2] Such inhibitors could be useful for probing fundamental pathways in cell biology ("chemical genetics"[3]), and for therapeutic applications. Creation of the desired inhibitors represents a considerable challenge because protein−protein interactions often involve large complementary surfaces on each partner. Recent efforts have shown that large interaction surfaces can be mimicked by medium-sized peptides,[2a−g] but these peptides may not be useful in vivo because of proteolytic instability and difficulty crossing biological membranes. General strategies are not yet available for creating physiologically stable and bioavailable molecules that display extensive protein-mimetic surfaces, although recent work on oligomers with well-defined conformations ("foldamers")[4] may provide solutions to this problem.

Formation of an intermolecular α-helical coiled-coil represents one of the simplest specific protein−protein interaction motifs.[5] Sequences that form α-helical coiled-coils display a recurring seven-residue pattern; the positions within this "heptad repeat" are conventionally designated a, b, c, d, e, f, and g. In the heptad pattern, hydrophobic residues such as leucine usually appear at the first and fourth positions (positions a and d). This periodicity allows the hydrophobic residues to be buried at the peptide−peptide interface when the α-helical coiled-coil forms. Electrostatic interactions involving residues at the fifth and seventh positions (e and g) of the heptad repeat contribute to specificity in α-helical coiled-coil formation. Specificity also arises from strategic placement of hydrophilic residues in a or d positions; these hydrophilic residues form polar contacts in the hydrophobic core of the dimeric state. Many transcription factors must dimerize via coiled-coil formation in order to bind to DNA and influence the rate of RNA synthesis.[5a,d] The regular appearance of leucine residues in transcription regulator sequences led to the phrase "leucine zipper"[6a] before these sequences were recognized to form α-helical coiled-coils,[6b] and both terms are now in regular use.

(1) Selected recent papers on protein−protein interactions: (a) Bogan, A. A.; Thorn, K. S. *J. Mol. Biol.* **1998**, *280*, 1. (b) Stites, W. E. *Chem. Rev.* **1997**, *97*, 1233. (c) Wells, J. A. *Proc. Natl. Acad. Sci. U.S.A.* **1996**, *93*, 1. (d) Jones, S.; Thornton, J. M. *Proc. Natl. Acad. Sci. U.S.A.* **1996**, *93*, 13.

(2) Selected recent papers on inhibition of protein−protein interactions: (a) Zutshi, R.; Brickner, M.; Chmielewski, J. *Curr. Opin. Chem. Biol.* **1998**, *2*, 62. (b) Schramm, H. J.; Boetzel, J.; Büttner, J.; Fritsche, E.; Göhring, W.; Jaeger, E.; König, S.; Thumfart, O.; Wenger, T.; Nagel, N. E.; Schramm, W. *Antiviral Res.* **1996**, *30*, 155. (c) Zutshi, R.; Fanciskovich, J.; Shultz, J.; Schweitzer, B.; Bishop, P.; Wilson, M.; Chmielewski, J. *J. Am. Chem. Soc.* **1997**, *119*, 4841. (d) Ghosh, I.; Chmielewski, J. *Chem. Biol.* **1998**, *5*, 439. (e) Prasanna, V.; Bhattacharjya, S.; Balaram, P. *Biochemistry* **1998**, *37*, 6883. (f) Gamboni, S.; Chaperon, C.; Friedrich, K.; Baehler, P. J.; Reymond, C. D. *Biochemistry* **1998**, *37*, 12189. (g) Judice, J. K.; Tom, J. Y. K.; Huang, W.; Wrin, T.; Vennari, J.; Petropoulos, C. J.; McDowell, R. S. *Proc. Natl. Acad. Sci. U.S.A.* **1997**, *94*, 13426. (h) Fan, X.; Flentke, G. R.; Rich, D. H. *J. Am. Chem. Soc.* **1998**, *120*, 8893. (i) Fairlie, D. P.; West, M. L.; Wong, A. K. *Curr. Med. Chem.* **1998**, *5*, 29. (j) Li, S.; Gao, J.; Satoh, T.; Friedman, T. M.; Edling, A. E.; Koch, U.; Choksi, S.; Han, X.; Korngold, R.; Huang, Z. *Proc. Natl. Acad. Sci. U.S.A.* **1997**, *94*, 73. (k) Tilley, J. W.; Chen, L.; Fry, D. C.; Emerson, S. D.; Powers, G. D.; Biondi, D.; Varnell, T.; Trilles, R.; Guthrie, R.; Mennona, F.; Kaplan, G.; LeMahier, R. A.; Carson, M.; Han, R.-J.; Liu, C.-M.; Palermo, R.; Ju, G. *J. Am. Chem. Soc.* **1997**, *119*, 7589. (l) Huang, J.; Schreiber, S. L. *Proc. Natl. Acad. Sci. U.S.A.* **1997**, *94*, 13396. (m) Hamuro, Y.; Calama, M. C.; Park, H. S.; Hamilton, A. D. *Angew. Chem., Int. Ed. Engl.* **1997**, *36*, 2680. For relatively small molecules that serve as agonists, i.e., that replace one of the protein partners in a specific protein−protein interaction, see: (n) Wrighton, N. C.; Farrell, F. X.; Chang, R.; Kashyap, A. K.; Barbone, F. P.; Mulcahy, R. P.; Johnson, D. L.; Barrett, R. W.; Jolliffe, L. K.; Dower, W. J. *Science* **1996**, *273*, 458. (o) Tian, S.-S.; Lamb, P.; King, A. G.; Miller, S. G.; Kessler, L.; Luengo, J. I.; Averill, L.; Johnson, R. K.; Gleason, J. G.; Pelus, L. M.; Dillon, S. B.; Rosen, J. *Science* **1998**, *281*, 257.

(3) Schreiber, S. L. *Bioorg. Med. Chem.* **1998**, *6*, 1127.

(4) Gellman, S. H. *Acc. Chem. Res.* **1998**, *31*, 173.

(5) Leading references on α-helical coiled-coil structure: (a) Lupas, A. *Trends Biochem. Sci.* **1996**, *21*, 375. (b) Hodges, R. S. *Biochem. Cell Biol.* **1996**, *74*, 133. (c) Alber, T. *Curr. Opin. Genet. Dev.* **1992**, *2*, 205. (d) O'Shea, E. K.; Rutkowski, R.; Kim, P. S. *Cell* **1992**, *68*, 699. (e) Schneider, J. P.; Lear, J. D.; DeGrado, W. F. *J. Am. Chem. Soc.* **1997**, *119*, 5742.

We would like to identify non-peptide inhibitors of leucine zipper formation because such molecules could exert control over gene expression.[7] Since α-helical coiled-coil interactions are widespread in biological systems, success with any particular target could lead to a general strategy with broad applications. A crucial first step toward our goal is development of a convenient and sensitive assay for leucine zipper dimerization. Fluorescence-based techniques provide powerful strategies for detecting specific intermolecular interactions in solution,[8] and several groups have examined leucine zipper formation by fluorophore-bearing peptides.[9,10] Here we describe the development of a fluorescence assay for homodimerization of a peptide corresponding to the leucine zipper region of the Jun oncoprotein. In the course of this work, we have found that several commonly employed fluorophores induce unwanted behavior when attached to a leucine zipper peptide, and that one prior report[10] on fluorescence-based detection of leucine zipper dimerization requires reinterpretation.

Results

Design. The Jun oncoprotein is a transcription factor that must either homodimerize or form a heterodimer with the Fos oncoprotein in order to bind to a target DNA site.[11] The Fos–Jun interaction is stronger than the Jun–Jun interaction; Fos–Fos interaction is weaker than Jun–Jun.[11b] We selected Jun–Jun dimerization as an initial target for inhibition based on the three considerations. First, this protein–protein recognition process is linked to human cancer. Second, Jun–Jun dimerization is relatively weak, which should facilitate initial discovery of inhibitors. Optimization of existing inhibitors and extrapolation to other leucine zippers is likely to be more straightfoward than identification of the first inhibitors. Third, Fos peptides provide positive controls. The fact that Fos homodimerization is weak suggests that this sequence will provide clues for designing leucine zipper antagonists that do not strongly self-associate.

Patel et al. have used fluorophore-labeled polypeptides derived from the Fos and Jun proteins (fragments of 72 and 109 residues, respectively) to examine heterodimer formation and heterodimer–DNA interaction.[9a] For both polypeptides, the fluorophore was attached to a unique cysteine residue located in the DNA-binding domain. We seek a minimal system focused exclusively on the protein–protein interaction for our initial search for dimerization inhibitors, and we therefore wanted to dispense with the DNA-binding domains. A system described by García-Echeverría in 1994[10] seemed to represent a useful prototype. García-Echeverría attached a 1-pyrenebutyryl unit,

along with a diglycine spacer, to the N-terminus of a leucine zipper peptide derived from the Max[12] transcription factor (this peptide is designated PyrGG-**3** here). When two pyrene units are held in proximity, they display a characteristic excimer emission at ca. 490 nm upon excitation at 350 nm. García-Echeverría observed the excimer emission for PyrGG-**3** and concluded that this peptide forms a leucine zipper dimer in solution.[10]

Pyrene as Fluorophore. Based on the reported behavior of PyrGG-**3**, derived from the leucine zipper region of Max,[10] we prepared **1** and PyrGG-**1** (Chart 1). Peptide **1** corresponds to residues 276–315 of the Jun protein (the leucine zipper region) in humans and several other vertebrates,[11] except that methionine-300 has been replaced by alanine. This modification was made to avoid complications from adventitious methionine oxidation. Residue 300 is at the b position of its heptad, which is far from the partner peptide in the leucine zipper dimer. Both methionine and alanine have high α-helix propensities;[13] therefore, the methionine → alanine mutation is not expected to affect leucine zipper dimerization. A second modification of **1** relative to Jun is the addition of an Ala-Ala-Tyr segment at the C-terminus; the tyrosine allows determination of peptide concentration via optical measurements.

Peptide **1** behaves as expected, according to circular dichroism (CD) and analytical ultracentrifugation. (All data reported here were obtained at room temperature in a common aqueous buffer, 100 mM NaCl, 10 mM phosphate, pH 7, unless otherwise indicated.) CD signals in the far-UV region arise largely from backbone amide groups, and these data provide insight on secondary structure; α-helix formation is associated with minima at 208 and 222 nm.[14] The CD data for **1** indicate substantial α-helicity at 50 μM.[15] Sedimentation equilibrium data for 50 μM **1**, spun at 36 K rpm (Figure 1), can be modeled by assuming that there is a dynamic mixture of two species with molecular weights of 4650 and 9350, with an association constant of 6.5 × 10^{-6} M^{-1}. The molecular weight of monomeric **1** is 4509, and the sedimentation data therefore suggest that **1** equilibrates between monomeric and dimeric states under these conditions. This type of equilibration is consistent with leucine zipper formation.

Like **1**, the pyrene-modified peptide PyrGG-**1** is highly α-helical at 50 μM, according to CD data.[15] A 50 μM solution of PyrGG-**1** displays the expected excimer emission at 488 nm upon excitation at 350 nm.[15] This excimer band indicates that pyrene units of different PyrGG-**1** molecules are held near one another under these conditions. These CD and fluorescence data for PyrGG-**1** parallel those reported by García-Echeverría for the Max-derived leucine zipper peptide PyrGG-**3**.[10]

Analytical ultracentrifugation reveals that the appended pyrene unit exerts a profound effect on the behavior of PyrGG-**1**, relative to **1**. Figure 2 shows sedimentation equilibrium data for 50 μM PyrGG-**1**, spun at 6000 rpm. These data are not consistent with dimer formation; instead, the data show that PyrGG-**1** forms large aggregates. Nonlinear analysis of these data and data obtained at other rotor speeds suggests that there is a broad distribution of aggregate sizes, with an average of ca. 80 molecules per aggregate, under these conditions. We

(6) (a) Landschulz, W. H.; Johson, P. R.; McKnight, S. L. *Science* **1988**, *240*, 1759. (b) O'Shea, E. K.; Rutkowski, R.; Kim, P. L. *Science* **1989**, *243*, 538.

(7) (a) Gottesfeld, J. M.; Neely, L.; Trauger, J. W.; Baird, E. E.; Dervan, P. B. *Nature* **1997**, *387*, 202. (b) Dickinson, L. A.; Gulizia, R. J.; Trauger, J. W.; Baird, E. E.; Mosier, D. E.; Gottesfeld, J. M.; Dervan, P. B. *Proc. Natl. Acad. Sci. U.S.A.* **1998**, *95*, 12890.

(8) Hermanson, G. T. *Bioconjugate Techniques*; Academic Press: San Diego, CA, 1996; Chapter 8.

(9) (a) Patel, L. R.; Curran, T.; Kerppola, T. K. *Proc. Natl. Acad. Sci. U.S.A.* **1994**, *91*, 7360. (b) Wendt, H.; Baici, A.; Bosshard, H. R. *J. Am. Chem. Soc.* **1994**, *116*, 6973. (c) Wendt, H.; Berger, C.; Baici, A.; Thomas, R. M.; Bosshard, H. R. *Biochemistry* **1995**, *34*, 4097. (d) Wendt, H.; Leder, L.; Härmä, H.; Jelesarov, I.; Baici, A.; Bosshard, H. R. *Biochemistry* **1997**, *36*, 204. (e) Dürr, E.; Jelesarov, I.; Bosshard, H. R. *Biochemistry* **1999**, *38*, 870. (f) Sosnick, T. R.; Jackson, S.; Wilk, R. R.; Englander, S. W.; DeGrado, W. F. *Proteins Struct. Funct. Genet.* **1996**, *24*, 427.

(10) García-Echeverría, C. *J. Am. Chem. Soc.* **1994**, *116*, 6031. (For related studies, see: García-Echeverría, C. *Lett. Pept. Sci.* **1994**, *1*, 255. García-Echeverría, C. *Bioorg. Med. Chem. Lett.* **1996**, *6*, 229.)

(11) For leading references, see: (a) Angel, P.; Karin, M. *Biochim. Biophys. Acta* **1991**, *1072*, 129. (b) O'Shea, E. K.; Rutkowski, R.; Stafford, W. F.; Kim, P. S. *Science* **1989**, *245*, 646.

(12) (a) Ferré-D'Amaré, A. R.; Prendergast, G. C.; Ziff, E. B.; Burley, S. K. *Nature* **1993**, *363*, 38. (b) The Max protein also engages in physiologically important heterodimer formation: Grandori, C.; Eisenman, R. N. *Trends Biochem. Sci.* **1997**, *22*, 177.

(13) O'Neil, K. T.; DeGrado, W. F. *Science* **1990**, *250*, 646, and references therein.

(14) Johnson, W. C. *Annu. Rev. Biophys. Biophys. Chem.* **1988**, *17*, 145, and references therein.

(15) Data may be found in the Supporting Information.
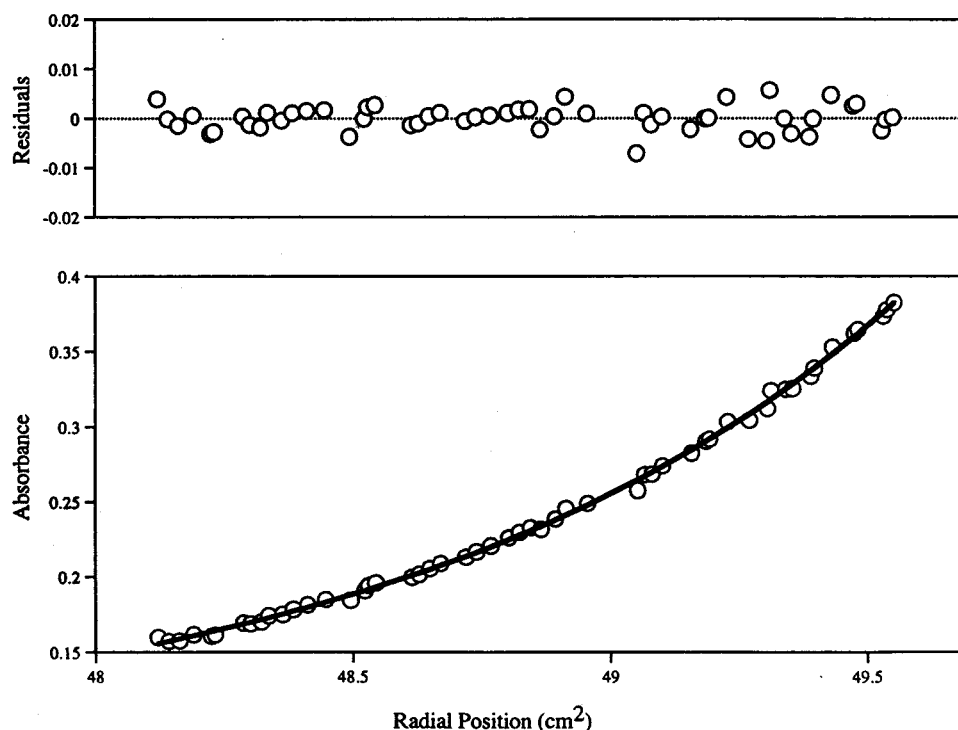
Figure 1. Analysis of sedimentation equilibrium data for 50 μM **1** (36K rpm). The circles are observed data and the line was generated by a nonlinear least-squares fit of the data based on the concentration distribution of an ideal system; this model assumes two noninteracting species. Molecular weight values of 4650 and 9350 (calculated for monomer, 4509) were obtained in 100 mM NaCl, 10 mM phosphate, pH 7.0, at 20 °C.

Chart 1

<div align="center">

PEPTIDE STRUCTURES

1 = Ac-RIARLEEKVKTLKAQNSELASTANALREQVAQLKQKVAAY-NH$_2$

PyrGG-**1** = 1-Pyrenebutyroyl-GGRIARLEEKVKTLKAQNSELASTANALREQVAQLKQKVAA-NH$_2$

PyrGG-**2** = 1-Pyrenebutyroyl-GGLEEKVKTLKAQNSELASTANALREQVA-NH$_2$

FluGG-**1** = Fluoresceinyl-GGRIARLEEKVKTLKAQNSELASTANALREQVAQLKQKVAA-NH$_2$

DecGG-**1** = 7-Diethylaminocoumarin-3-carboyl-GGRIARLEEKVKTLKAQNSELASTANALREQVAQLKQKVAA-NH$_2$

HcGG-**1** = 7-Hydroxycoumarin-3-carboyl-GGRIARLEEKVKTLKAQNSELASTANALREQVAQLKQKVAA-NH$_2$

3 = Ac-RRKVDTLQQDIDDLKRQVALLEQQVRALE-NH$_2$

PyrGG-**3** = 1-Pyrenebutyroyl-GGRRKVDTLQQDIDDLKRQVALLEQQVRALE-NH$_2$

PyrGG-**4** = 1-Pyrenebutyroyl-GGVLDRRKDTILRQDLDKRQLAVEQQQEAVL-NH$_2$

5 = GGRIARLEEKVKTLKAQNSELASTY-NH$_2$

FluGG-**5** = Fluoresceinyl-GGRIARLEEKVKTLKAQNSELASTY-NH$_2$

DecGG-**5** = 7-Diethylaminocoumarin-3-carboyl-GGRIARLEEKVKTLKAQNSELASTY-NH$_2$

HcGG-**5** = 7-Hydroxycoumarin-3-carboyl-GGRIARLEEKVKTLKAQNSELASTY-NH$_2$

**6** = Ac-LTDTLQAETDQLEDKKSALQTEIANLLKEKEKLELILAAY-NH$_2$

7 = Ac-ETDQLEDKKSALQTEIANLLKEKEKLELILAAY-NH$_2$

8 = Ac-KKSALQTEIANLLKEKEKLELILAAY-NH$_2$

</div>

evaluated the distribution for the data shown in Figure 2 by analyzing small portions of the plot. A linear fit of the data between 48.0 and 48.2 cm^2 suggests a 63-mer, and a linear fit of the data between 50.4 and 50.7 cm^2 suggests a 178-mer. Thus, attachment of a pyrene unit to the N-terminus of the Jun leucine zipper sequence leads to high-order aggregation. PyrGG-**1** exists as a monomer in 8 M guanidinium chloride, according to sedimentation equilibrium data.[15]

We probed the importance of peptide size for pyrene-induced aggregation by examining PyrGG-**2**, which shares the central sequence of PyrGG-**1** but lacks the four N-terminal residues and the eight C-terminal residues. CD data for 50 μM PyrGG-**2**[15] indicate that there is relatively little α-helicity under these conditions. No pyrene excimer emission is observed upon excitation at 350 nm for 50 μM PyrGG-**2**, but strong excimer emission at 488 nm is observed at 500 μM peptide.[15] These
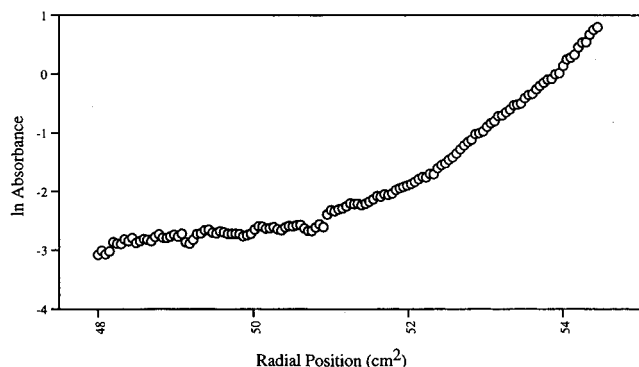
Figure 2. Plot of ln absorbance vs (radial distance)^2 for 50 μM PyrGG-**1** at equilibrium (6K rpm) in 100 mM NaCl, 10 mM phosphate, pH 7.0, at 20 °C. These data indicate the presence of a distribution of large molecular weight species with an average molecular weight of 379 700 (calculated for monomer, 4691).
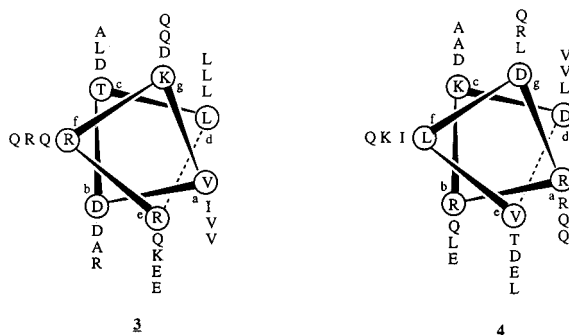
Figure 3. Helical wheel diagrams for peptides **3** and **4** (the latter corresponds to PyrGG-**4** without the N-terminal pyrene-diglycine segment). Lowercase letters (a–g) refer to the seven positions in the heptad pattern found in sequences that form α-helical coiled coils. Uppercase letters refer to the amino acid residues, according to the usual convention.
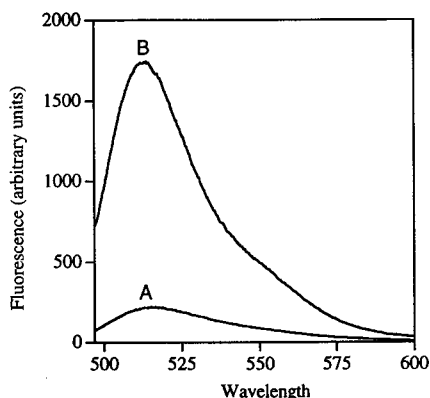
Figure 4. Fluorescence emission spectra (λ_{ex} = 492 nm) in 100 mM NaCl, 10 mM phosphate, pH 7.0: A, 5 μM FluGG-**1**; B, 5 μM fluorescein.

data suggest that PyrGG-**2** does not self-associate at 50 μM, but that self-association occurs when the concentration is raised.

Analytical ultracentrifugation data for PyrGG-**2** are consistent with the fluorescence data in suggesting that aggregation occurs at 500 μM but not at 50 μM. Sedimentation equilibrium results indicate that the peptide is monomeric at 50 μM; a distribution of aggregates is formed at 500 μM, with an average of ca. 11 molecules per aggregate.[15] Most of the 12 residues removed from PyrGG-**1** to produce PyrGG-**2** are either hydrophilic (two lysines, two arginines, and two glutamines) or neutral (three alanines); indeed, the truncation removes +4 in total peptide

charge (PyrGG-**1** should have a net charge of +5 at pH 7, while PyrGG-**2** should have a net charge of +1). Therefore, the diminished propensity for aggregation of PyrGG-**2** relative to PyrGG-**1** suggests that the appended pyrene does not promote high-order aggregation simply by increasing net hydrophobicity, because PyrGG-**2** has a larger net hydrophobicity than does PyrGG-**1**.

We reexamined Max-derived peptides **3** and PyrGG-**3**[10] in light of our discovery that an N-terminal pyrene unit induces high-order aggregation of the Jun leucine zipper sequence. As previously reported,[10] 40 μM PyrGG-**3** displays a strong α-helical CD signature in 100 mM NaCl, 10 mM phosphate buffer, pH 7.0.[15] Under the same conditions, excitation at 350 nm leads to pyrene excimer emission at 488 nm.[15,16] Sedimentation equilibrium data for 50 μM PyrGG-**3**, spun at 12 000 rpm, show that large aggregates form under these conditions.[15] Nonlinear analysis of these data and data obtained at lower rotor speeds suggest a broad distribution of aggregate sizes, with an average of ca. 40 molecules per aggregate. (Analytical ultracentrifugation was not performed in the original study of PyrGG-**3**.) In contrast, peptide **3**, lacking the N-terminal pyrene unit, equilibrates between monomeric and dimeric forms at 50 μM, according to sedimentation equilibrium data.[15] CD data show substantial α-helicity for 50 μM **3**.[15] Thus, as shown above for the Jun-derived leucine zipper, the attachment of a 1-pyrene-butyryl unit to the Max-derived leucine zipper sequence induces high-order aggregation.

Why does addition of a terminal pyrene unit cause such a dramatic alteration in peptide self-association? García-Echeverría previously reported that 1-pyrenebutyrate (<100 μM) does not aggregate under the solvent conditions used here,[10,17] which suggests that the pyrene unit alone is not the source of the change. We probed the role of the peptide portion in the aggregation process by examining PyrGG-**4**, an isomer of PyrGG-**3** in which the amino acid sequence is scrambled. Figure 3 compares the sequences **3** and **4** in an α-helical conformation, with the view along the helix axis; this perspective highlights the distribution of hydrophilic and hydrophobic residues around the helix perimeter. The sequence of **3** is typical of leucine zipper peptides: there is a recurring pattern in which leucine appears every seven residues (a position), and the fourth residue after each leucine (d position) is also hydrophobic, valine or isoleucine. Figure 3 shows that the sequence of PyrGG-**4** has been scrambled, destroying the heptad pattern.

CD data for 40 μM PyrGG-**4** indicate that this peptide displays little α-helicity and is predominantly in the random coil state.[15] Fluorescence data for 50 μM PyrGG-**4** reveal a total absence of pyrene excimer emission.[15] Sedimentation equilibrium data for 50 μM PyrGG-**4** suggest an exclusively mono-meric state.[15] Thus, all three physical measurements agree that PyrGG-**4** behaves very differently from isomer PyrGG-**3**. These results, along with the comparison Jun-derived peptides PyrGG-**1** and PyrGG-**2** presented above, demonstrate that attaching a pyrene unit to a peptide does not automatically lead to

(16) In ref 10, fluorescence data for PyrGG-**1** were obtained in 4:1 10 mM phosphate buffer:DMSO. We obtained all data (CD, fluorescence, and sedimentation) for PyrGG-**1** and other peptides in an aqueous buffer, 10 mM phosphate buffer, pH 7, to facilitate comparison. We found that fluorescence data obtained in the aqueous buffer were qualitatively similar to fluorescence data we obtained in 4:1 10 mM phosphate buffer:DMSO.

(17) We have corroborated the behavior of pyrenebutryate reported in ref 10, for 4:1 10 mM phosphate buffer:DMSO. Further, we find no evidence of pyrene excimer emission from a ca. 40 μM pyrenebutyrate solution (near the solubility limit) in aqueous buffer (10 mM phosphate, pH 7). The observation that pyrenebutyrate does not aggregate avidly in aqueous solution is consistent with previous data on pyrenesulfonate: Menger, F. M.; Whitesell, L. G. *J. Org. Chem.* **1987**, *52*, 3793.

aggregation. The high-order aggregation observed for PyrGG-**1** and PyrGG-**3** must arise from cooperativity between the pyrene unit and the leucine zipper peptide segment.

Fluorescein as Fluorophore. In our search for a nonperturbing fluorophore, we turned to fluorescein because Wendt et al. have attached this unit to the N-terminus of several leucine zipper peptides, via a triglycine spacer.[9b−e] These fluorescently labeled peptides were used to examine the mechanism of leucine zipper dimerization. Fluorescein is a self-quenching species, and self-association of labeled peptides is therefore indicated by a decrease in fluorescence. One study by Wendt et al. involved the leucine zipper sequence of the transcription factor GCN4;[9b] these workers concluded that this peptide undergoes monomer/dimer equilibration over the range 0.5−4.0 μM based on the concentration dependence of fluorescence quenching. A similar approach was used by Wendt et al. to establish monomer−dimer equilibration for a series of designed fluorescent leucine zipper peptides.[9c]

We prepared FluGG-**1**, the Jun leucine zipper sequence with an N-terminal fluorescein unit and a diglycine spacer, in order to determine whether fluorescein influences peptide self-association. Far-UV CD data for FluGG-**1** suggest a high degree of α-helicity at 50 μM, comparable to the extent of α-helix formation observed for **1** and PyrGG-**1**.[15] Figure 4 compares the fluorescence of 5 μM FluGG-**1** and 5 μM fluorescein upon excitation at 492 nm. Both samples display emission bands at 514 nm, but the intensity of the emission of FluGG-**1** is greatly diminished relative to fluorescein, which suggests that the fluorescein units attached to the peptide are held near one another. We probed the stoichiometry of FluGG-**1** self-association by analytical ultracentrifugation.[15] At 50 μM FluGG-**1** the sedimentation equilibrium data could be analyzed by assuming the presence of a single species, corresponding to a tetramer. Thus, we conclude that a fluorescein appendage, like a pyrene appendage, induces higher order aggregation of the normally dimeric Jun leucine zipper, although fluorescein exerts a weaker aggregation-promoting effect than does pyrene.

7-Diethylaminocoumarin as Fluorophore. We turned to a fluorescent label of lower molecular weight than pyrene or fluorescein in the hope of diminishing the perturbing effects of the attached fluorophore on leucine zipper formation. Wendt et al. used 7-dimethylaminocoumarin-4-acetic acid for N-terminal acylation of leucine zipper peptides in order to examine heterodimer formation, via fluorescence resonance energy transfer between the coumarin donor and a fluorescein acceptor.[9c] Coumarins can also be used to examine homodimerization because, like fluorescein, coumarins are self-quenchers.

We used 7-diethylaminocoumarin-3-carboxylic acid to prepare Jun-derived leucine zipper peptide DecGG-**1**. Far-UV CD data for 50 μM DecGG-**1** show considerable α-helix formation,[15] with the extent comparable to that observed for FluGG-**1**. Upon excitation of 50 μM DecGG-**1** or 50 μM 7-diethylaminocoumarin at 420 nm, both samples display emission bands at 473 nm; however, DecGG-**1** shows a much less intense emission than does the fluorophore alone.[15] This difference suggests that DecGG-**1** self-associates in a manner that places fluorophores close to one another (e.g., leucine zipper formation). Sedimentation equilibrium data for 50 μM DecGG-**1** could be analyzed by assuming the presence of a single species, corresponding to a dimer.[15] This result suggests that the 7-diethylaminocoumarin unit stabilizes the dimeric state of DecGG-**1** because, as discussed above, sedimentation data for 50 μM **1** indicate a dynamic equilibrium between monomeric and dimeric forms.
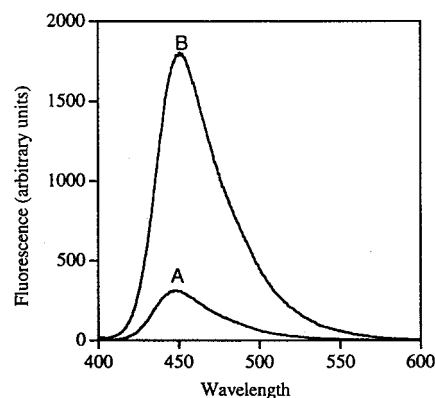

Figure 5. Fluorescence emission spectra (λ_{ex} = 386 nm) in 100 mM NaCl, 10 mM phosphate, pH 7.0: A, 50 μM HcGG-**1**; B, 50 μM 7-hydroxycoumarin.

We prepared a truncated peptide bearing the N-terminal 7-diethylaminocoumarin unit in order to probe the extent of this fluorophore's stabilization of the dimer. The peptide portion of DecGG-**5** contains 22 residues from Jun, corresponding to the first three heptads from the leucine zipper region. Peptide **5** itself appears to be largely random coil by CD up to 1 mM, as does DecGG-**5** at a similar concentration.[15] Sedimentation data indicate that DecGG-**5** is monomeric at 50 μM.[15] Surprisingly, however, the fluorescence of 50 μM DecGG-**5** is considerably diminished relative to 50 μM 7-diethylaminocoumarin-3-carboxylic acid.[15]

The weak fluorescence of monomeric DecGG-**5** suggests that there is an intramolecular fluorescence quenching mechanism at work in this peptide. We suspect that the peptide folds around the relatively hydrophobic fluorophore. The folding hypothesis is supported by the observation that the fluorescence of DecGG-**5** increases upon heating or addition of GdmCl,[15] both of which are expected to cause unfolding. A terminal fluorescein unit also appears to be susceptible to intramolecular quenching, since FluGG-**5** shows similar behavior to that described for DecGG-**5**.

7-Hydroxycoumarin as Fluorophore. Although 7-diethylaminocoumarin was superior to either pyrene or fluorescein in terms of influence on the self-association of the Jun leucine zipper sequence, we continued our quest for a nonperturbing fluorophore because 7-diethylaminocoumarin strongly stabilizes the dimeric state. 7-Hydroxycoumarin-3-carboxylic acid was an attractive choice as N-terminal tag because this unit is expected to bear a negative charge at neutral pH, which should prevent a strong intrinsic attraction between neighboring 7-hydroxycoumarin moieties. Like 7-diethylaminocoumarin, 7-hydroxycoumarin is a self-quencher. 7-Hydroxycoumarin-3-carboxylic acid was used to prepare Jun-derived leucine zipper peptide HcGG-**1**.

Far-UV CD data indicate that 50 μM HcGG-**1** is highly α-helical, comparable to DecGG-**1** and other derivatives of this peptide.[15] Figure 5 compares the fluorescence of 50 μM HcGG-**1** and 50 μM 7-hydroxycoumarin upon excitation at 386 nm. The peptide emission is greatly diminished relative to the fluorophore alone, suggesting peptide self-association. Analytical ultracentrifugation of 50 μM HcGG-**1** suggests a dynamic equilibrium between monomeric and dimeric states, with an association constant of 4.2×10^{-5} M^{-1}.[15] This behavior is similar to that of 50 μM **1**, although the apparent association constant for HcGG-**1** is roughly 6-fold larger than for **1**. Thus, 7-hydroxycoumarin exerts only minimal influence on leucine zipper formation, and this unit is clearly the most suitable among the
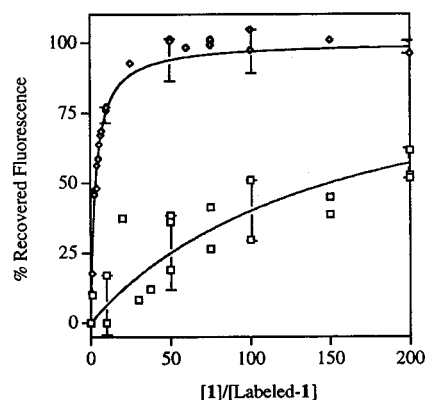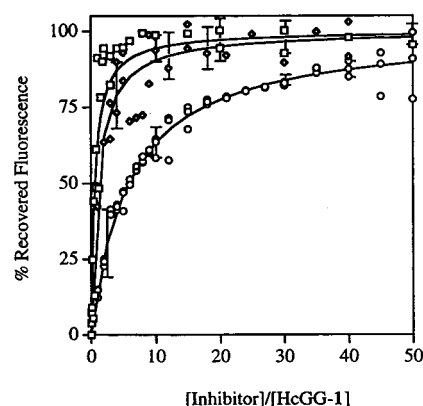
Figure 6. Titrations of HcGG-**1** (diamonds) and DecGG-**1** (squares) with **1** in aqueous solution (100 mM NaCl, 10 mM phosphate, pH 7.0). Solid lines are fits of the experimental data as described in the Experimental Section. Representative error bars, based on multiple independent measurements, are shown. Measurements were made within 5−10 min of sample preparation; however, no change was observed when the time was increased to several hours.

four common fluorophores we have examined for creation of a fluorescence-based leucine zipper dimerization assay.

Monitoring Jun Leucine Zipper Disruption by Unlabeled Jun and Fos Peptides. Our initial evaluation of a fluorescence-based leucine zipper inhibitor assay involved the use of **1** to disrupt the dimer of HcGG-**1** or DecGG-**1**. Figure 6 shows the effect of increasing concentrations of **1** on the fluorescence observed for 5 μM HcGG-**1** or DecGG-**1**. In both cases, addition of **1** causes an increase in observed fluorescence, as expected if fluorophore-**1** conjugates are partitioning from homodimers (in which proximal fluorophores cause quenching) to heterodimers (in which each fluorophore displays maximum fluorescence). A large excess of **1** leads to a maximum fluorescence intensity that is ca. 10-fold larger than observed for 5 μM fluorophore-**1** conjugate.

Unlabeled peptide **1** disrupts DecGG-**1** less effectively than it disrupts HcGG-**1**; the molar excess of **1** required for 50% maximal fluorescence is 150 for DecGG-**1** and 3.2 for HcGG-**1**. This difference is consistent with analytical ultracentrifugation results discussed above, which showed that the DecGG-**1** dimer is more stable than the HcGG-**1** dimer. The data in Figure 6 suggest that the attached 7-hydroxycoumarin unit modestly promotes peptide dimerization; if HcGG-**1** had no effect on leucine zipper dimer stability, then 1 equiv of **1** should produce 50% maximal fluorescence. This modest stabilization of dimeric HcGG-**1** relative to **1** is consistent with analytical ultracentrifugation results provided above. The stabilizing effect of the N-terminal 7-hydroxycoumarin unit is substantially smaller than the stabilizing effect of the N-terminal 7-diethylaminocoumarin unit.

We used leucine zippers derived from the Fos sequence for further evaluation of the dimerization inhibitor assay based on HcGG-**1**. Peptide **6** corresponds to the leucine zipper domain of Fos from murine osteosarcoma virus[11] with two minor modifications. First, a tyrosine residue has been attached to the C-terminus, to allow concentration determination by optical measurements (the preceding two alanine residues are part of the Fos sequence). Second, a phenylalanine near the C-terminus (the c position of the final heptad) has been changed to leucine to avoid interference with tyrosine-based concentration determinations. Analytical ultracentrifugation indicates that **6** does not self-associate at 50 or 100 μM.[15] (In contrast, a peptide nearly identical to **6** has been reported to sediment as a dimer at 40 μM and 4 °C.[11b]) Figure 7 shows the effect of increasing

Figure 7. Titrations of HcGG-**1** with **6** (squares), **7** (diamonds), and **8** (circles) in aqueous solution (100 mM NaCl, 10 mM phosphate, pH 7.0). Solid lines are fits of the experimental data as described in the Experimental Section. Representative error bars, based on multiple independent measurements, are shown. Measurements were made within 5−10 min of sample preparation; however, no change was observed when the time was increased to several hours.

concentrations of **6**, and two shorter analogues, **7** and **8**, on the fluorescence observed for 5 μM HcGG-**1**. The full-length Fos leucine zipper sequence, **6**, is more effective at disrupting the HcGG-**1** dimer than is the full-length Jun leucine zipper, **1**. This behavior is consistent with other reports that Fos−Jun affinity is higher than Jun−Jun.[11b] For **6**, 0.6 equiv is required to produce 50% maximal fluorescence, while, as noted above, 3.2 equiv of **1** is required for a similar effect (i.e., ca. 5-fold superiority of **6** relative to **1**).

Data for truncated Fos peptides **7** and **8** (Figure 7) show that substantial affinity for Jun remains even when a significant proportion of the Fos sequence is removed. In **7**, the 7 N-terminal residues of **6** have been omitted, while the 14 N-terminal residues have been omitted in **8**. For **7**, 1.1 equiv is required to produce 50% maximal fluorescence, and 5.8 equiv of **8** is required to achieve this effect. Thus, these truncated Fos peptides show affinities for Jun that are comparable to that of Jun itself. Truncation of Fos by another seven residues drastically reduces affinity for Jun, to a negligible level (not shown).

Discussion

Assay Development. We have shown that attachment of an N-terminal 7-hydroxycoumarin fluorophore to the Jun leucine zipper sequence (HcGG-**1**) allows a convenient and quantitative assay for disruption of the Jun−Jun homodimer. In the dimeric state, the fluorophores are held near enough to one another to cause self-quenching of fluorescence. When an unlabeled competitor peptide is added, heterodimer formation causes separation of fluorophores from one another, which is signaled by an increase in fluorescence. The number of equivalents of competitor peptide required to produce 50% of the maximum fluorescence from the HcGG-**1** correlates with the affinity of the competitor peptide for the Jun leucine zipper.

The fluorescence assay based on HcGG-**1** should allow rapid screening of potential inhibitors, peptide or nonpeptide, of Jun−Jun dimerization. Extension of this approach to other α-helical coiled coil dimers, including heterodimers, is expected to be straightforward. For example, we could screen for inhibitors of Fos−Jun dimerization by placing 7-hydroxycoumarin at the N-terminus of both Fos and Jun leucine zipper peptides. In this particular example, the sensitivity of the assay might be diminished if the inhibitor bound to the Fos segment, since

liberated Jun peptide would homodimerize, leading to self-quenching of the attached fluorophores. However, even if the maximum signal corresponded to only half of the total fluorophore (the proportion attached to the Fos peptide), sensitivity would be sufficient for a useful screen.

HcGG-**1** and related fluorogenic peptides should be useful for screening resin-bound combinatorial libraries of potential inhibitors generated by the split-mix strategy. In this scenario, each resin bead contains a single molecule; if the attached molecule binds the Jun leucine zipper, then the bead should become fluorescent when exposed to a solution containing HcGG-**1**. Any HcGG-**1** that does not bind to an immobilized molecule should remain in solution in the homodimer form, which displays little fluorescence. Fluorescent beads can be isolated manually or with a fluorescence-activated cell sorter. Once inhibitor candidates are identified, by screening of soluble or immobilized molecules, more detailed analysis would be required to determine whether leucine zipper disruption detected via this simplistic assay corresponds to interference with gene regulation.

Unintended Effects of Fluorophore Attachment. Our results demonstrate that attachment of commonly employed fluorophores can profoundly alter leucine zipper behavior. The most dramatic effect is exerted by pyrene, which induces high-order aggregation of peptides derived from the leucine zipper regions of Jun and Max; indeed, analytical ultracentrifugation data reported here show that previous conclusions regarding the behavior of Max-derived peptide PyrGG-**3** are incorrect.[10] Fluorescein also induces self-association beyond the dimer state, although this fluorophore is less perturbing than is pyrene. Neither of the coumarin fluorophores examined causes high-order aggregation of the Jun leucine zipper sequence, but both coumarins appear to stabilize the Jun–Jun dimer. Dimer stabilization is more profound for 7-diethylaminocoumarin than for 7-hydroxycoumarin, and this difference has led us to select 7-hydroxycoumarin for further studies. Dimer stabilization by the attached fluorophore may lead to false negative results for weak inhibitors of leucine zipper formation, but this relatively minor effect does not invalidate the assay. In contrast, the high-order aggregation induced by pyrene or fluorescein could lead to unacceptably large distortions in the screening of dimerization inhibitors.

Why does fluorophore attachment alter the behavior of leucine zipper peptides? In each case, the alteration presumably results from a favorable fluorophore–fluorophore interaction, perhaps involving the hydrophobic effect. However, careful examination of pyrene, the most perturbing appendage, clearly demonstrates that fluorophore–fluorophore interaction alone is not sufficient to induce high-order aggregation. Several of the pyrene-bearing peptides we prepared do not self-associate at all.

The high-order aggregation of pyrene-functionalized leucine zipper peptides PyrGG-**1** and PyrGG-**3** must result from cooperativity between the peptide and pyrene moieties. This high-order aggregation requires a leucine zipper sequence, i.e., the heptad repeat of hydrophobic and hydrophilic residues that is characteristic of sequences that form α-helical coiled-coil dimers. Thus, specific peptide–peptide interactions, similar to those of α-helical coiled-coils, play an essential role in the high-order self-association of PyrGG-**1** and PyrGG-**3**. This conclusion is required by the lack of aggregation observed for PyrGG-**4**, the "scrambled" isomer of PyrGG-**3** that lacks the leucine zipper heptad pattern. The importance of peptide–peptide interactions is seen also in the decreased tendency to self-associate displayed by truncated peptide PyrGG-**2** relative to full-length PyrGG-**1**.
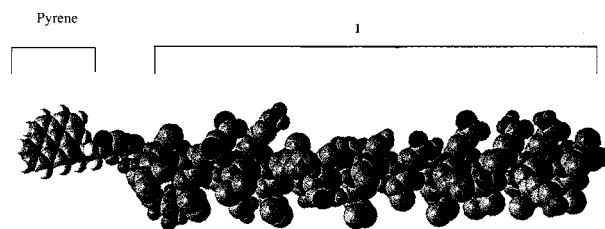
Figure 8. Space-filling model for PyrGG-**1**, showing the relative sizes of the peptide and pyrene segments. The peptide is modeled as a standard α-helix.

Since all of the peptides discussed here are amphiphilic, their behavior should be considered in the context of current views on the relationship between the topology and self-association modes of amphiphiles.[19] Figure 8 presents an idealized structure of PyrGG-**1**, with the peptide portion in an α-helical conformation. This image shows that introduction of the pyrene unit constitutes a relatively small perturbation of the total molecular surface. In light of this image, the pyrene appendage would not be expected to induce micelle-like aggregation in peptides such as PyrGG-**1** and PyrGG-**3** simply on the basis of added hydrophobicity.[19]

The perturbing effects we have detected in fluorophore-labeled leucine zipper peptides are relevant to the widespread interest in fluorescent derivatization of biopolymers, since it is commonly assumed that the attached fluorophore will serve as a nonperturbing reporter.[10,20] Our results suggest that this assumption should be tested directly on a case-by-case basis. Interestingly, studies involving fluorescently labeled[9b,c] or nonlabeled[18] GCN4-derived peptides have led to different conclusions regarding leucine zipper folding/dimerization kinetics. Zitzewitz et al.[18] used far-UV CD measurements, which probe global secondary structure, to examine leucine zipper formation; these workers reached somewhat different mechanistic conclusions from those of Wendt et al.,[9b,c] who used fluorescein-labeled peptides. Zitzewitz et al. suggested several possible sources of the discrepancy, one of which is that the fluorophore "may itself favor alternatively folded structures".

The synergy we detect between the pyrene and peptide units in promoting high-order aggregation is of interest in the context of recent efforts to engineer specific associations involving peptide segments.[21] Examples include "peptide amphiphiles" bearing long alkyl units,[21b] and peptide "maquettes" with porphyrin appendages.[21c,d] Analysis of these systems via analytical ultracentrifugation should provide useful information. Biological systems often append hydrophobic units to proteins via posttranslational modification.[22] These modifications are known to anchor proteins in biological membranes; it will be interesting to see whether Nature uses hydrophobic appendages to induce

(18) Zitzewitz, J. A.; Bilsel, O.; Luo, J.; Jones, B. E.; Matthews, C. R. *Biochemistry* **1995**, *34*, 12812.
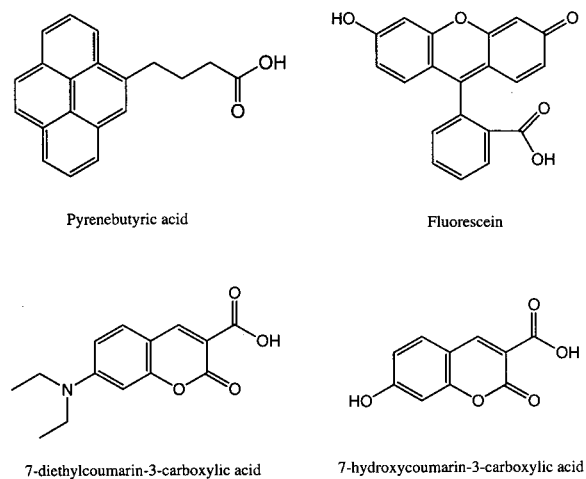
(19) Israelachvili, J. N.; Marcelja, S.; Horn, R. G. *Q. Rev. Biophys.* **1980**, *13*, 121.

(20) (a) Other examples of pyrene-functionalized peptides: Nishimo, H.; Mihara, H.; Tanaka, Y.; Fujimoto, T. *Tetrahedron Lett.* **1992**, *33*, 5767. Mihara, H.; Tanaka, Y.; Fujimoto, T.; Nishino, N. *J. Chem. Soc., Perkin Trans. 2* **1995**, 1133. (b) Peptides bearing other fluorophores: García-Echeverría, C. *Bioorg. Med. Chem. Lett.* **1997**, *7*, 1695. Mehta, S.; Meldal, M.; Ferro, V.; Duus, J. O.; Bock, K. *J. Chem. Soc., Perkin Trans. 1* **1997**, 1365.

(21) (a) Petka, W. A.; Harden, J. L.; McGrath, K. P.; Wirtz, D.; Tirrell, D. A. *Science* **1998**, *281*, 389. (b) Yu, Y.-C.; Berndt, P.; Tirrell, M.; Fields, G. B. *J. Am. Chem. Soc.* **1996**, *118*, 12515. (c) Sharp, R. E.; Diers, J. R.; Bocian, D. F.; Dutton, P. L. *J. Am. Chem. Soc.* **1998**, *120*, 7103. (d) Gibney, B. R.; Johansson, J. S.; Rabanal, F.; Skalicky, J. J.; Wand, A. J.; Dutton, P. L. *Biochemistry* **1997**, *36*, 2798.

(22) Zhang, F. L.; Casey, P. J. *Annu. Rev. Biochem.* **1996**, *65*, 241.

Chart 2

Pyrenebutyric acid

Fluorescein

7-diethylcoumarin-3-carboxylic acid

7-hydroxycoumarin-3-carboxylic acid

self-association in the absence of membranes, via processes similar to those we have observed.

Experimental Section

N-9-Fluorenylmethyloxycarbonyl amino acids were obtained from Advanced Chemtech (Louisville, KY). The arginine side chain was protected with the 4-methoxy-2,3,6-trimethylbenzenesulfonyl group. Glutamine and aparagine were protected as the γ-triphenylmethyl derivatives. Lysine was *tert*-butoxycarbonyl protected. Glutamic acid and aspartic acid were protected as *tert*-butyl esters. Tyrosine, threonine, and serine were protected as *tert*-butyl ethers. Water used for HPLC was Millipore grade. HPLC grade acetonitrile, HPLC grade *N,N*-dimethylformamide (DMF), trifluoroacetic acid (TFA), and pyrenebutyric acid were obtained from Aldrich (Milwaukee, WI). Diisopropylethylamine (DIEA), [2-(1-*H*-benzotriazolyl-1-yl)-*N,N,N′,N′*-tetramethyluronium hexafluorophosphate (HBTU), piperidine, and tetrahydrofuran (THF) were purchased from (Applied Biosystems, Foster City, CA). 7-Diethylaminocoumarin-3-carboxylic acid, 7-hydroxycoumarin-3-carboxylic acid, and fluorescein were obtained from Molecular Probes (Eugene, OR) (Chart 2).

Peptide Synthesis. All peptides were synthesized by standard solid-phase techniques with *N*-9-fluorenylmethyloxycarbonyl amino acids on 2,4-dimethoxybenzhydrylamine resin, which provides an amide terminal group upon cleavage. Couplings were performed on a 25 μmol scale on a Synergy 432A solid-phase peptide synthesizer (Applied Biosystems, Foster City, CA). Couplings were achieved by activation of 3 equiv of amino acid in DMF with HBTU and DIEA, followed by reaction with the piperidine-deprotected α-amino group on the peptide resin. THF was used as a secondary solvent to displace DMF and aid in drying of the resin bound peptide. Coupling times were approximately 25 min. This time was doubled for more difficult couplings. Extent of coupling was monitored by conductivity of the solution. Capping of peptides with all fluorophores (carboxylic acids) was achieved by methods similar to amino acid couplings on the automated peptide synthesizer; these capping steps were straightforward for all fluorophores.

Peptides not capped with fluorophores were acetylated by treatment with 100 μL acetic anhydride and 50 μL triethylamine in 350 μL DMF. The solvent mixture was washed through the cartridge over a period of 30 min. In all cases, the peptide was washed with 20–25 mL MeOH and dried with N_2.

Peptides were cleaved from the resin by stirring for 3 h in 2 mL TFA with 100 μL thioanisole and 50 μL ethanedithiol. The mixture was passed through a glass wool plug to filter out the resin and washed with approximately 2 mL additional TFA. The filtrate was concentrated to approximately 1 mL. The peptide was then precipitated with 20 mL of anhydrous ether, and the mixture was centrifuged to pellet the precipitate. The ether was decanted and discarded. The procedure was repeated three times, and the peptide was then dissolved in a minimum amount of water. The crude peptide was lyophilized.

Peptides were purified by reverse phase semipreparative HPLC using a Vydac 214TP510 C4-silica column. Solvent systems employed gradients formed by mixing 0.1% (v/v) TFA in H_2O and 0.1% (v/v) TFA in CH_3CN. Elution was monitored by absorbance at 220 nm. Flow rates were 3 mL/min. Peptide purities were determined with a Vydac 214TP54 C4-silica analytical column and found to be >95%; chromatograms and purification conditions for each peptide are available in the Supporting Information.

Circular Dichroism. CD spectra were obtained on an AVIV 62A DS CD spectrophotometer at 25 °C, with 1 nm bandwidth, 1 nm resolution, 0.1 mm path length, and a 5–10 s averaging time. Spectra were corrected by the subtraction of a blank corresponding to the solvent composition of each sample. Peptide concentrations were determined by UV absorbance at 275 nm, using an extinction coefficient of 1450 M^{-1} cm^{-1}, as previously determined for tyrosine in 6 M guanidine hydrochloride.[23]

Fluorescence measurements were made on a Hitachi F-4500 fluorescence spectrophotometer (Hitachi, Naperville, IL) with a 3 mm path length cuvette. A minimum volume of 110 μL was used. Spectra were measured in 0.2 nm steps at a rate of 2400 nm/min. Excitation and emission slit widths were both 5.0 nm. Excitation at 350 nm was used for pyrene-containing peptides, and the excimer emission maximum at 488 nm was monitored. Excitation at 492 nm was used for fluorescein-containing peptides, and the excimer emission maximum at 514 nm was monitored. Excitation at 420 nm was used for 7-diethylaminocoumarin-containing peptides, and the excimer emission maximum at 473 nm was monitored. Excitation at 386 nm was used for 7-hydroxycoumarin-containing peptides, and the excimer emission maximum at 448 nm was monitored. All emission spectra were recorded over the range 340–600 nm.

Competitive Binding Studies. Figures 6 and 7 show the increase in fluorescence that results from adding inhibitor peptides (no fluorophore) to solutions containing either HcGG-**1** or DecGG-**1**. These data were fit with the equation $F = F_{max}(C/(C_{50} + C))$, using the data analysis program Prizm (Graphpad Software, Inc. San Diego, CA). F is the fluorescence recovery observed after addition of a given amount of inhibitor peptide (no fluorophore); F is reported as a percentage of the maximal fluorescence recovery. F_{max} is the maximum fluorescence; this value was determined for HcGG-**1** and for DecGG-**1** as the limiting fluorescence in the presence of high concentrations of full-length Fos peptide **6**. C is the concentration of inhibitor added, and C_{50} is the concentration of inhibitor required to reach half-maximal fluorescence.

Analytical Ultracentrifugation. Centrifugation experiments were carried out with a Beckman Optima XL-A analytical ultracentrifuge equipped with an AN-60 rotor. Sample cells were assembled with 1.2 cm spacers, and each well contained 100 μL of sample. Samples were referenced against a blank corresponding to the solvent without peptide. Pyrene-containing samples were monitored by absorbance at 330 nm. 7-Diethylaminocoumarin-containing peptides were monitored by absorbance at 438 nm. 7-Hydroxycoumarin-labeled peptides were monitored by absorbance at 409 nm. All other peptides, including fluorescein-labeled peptides, were monitored at the tyrosine absorbance of 275 nm. Sedimentation was monitored at 2 h intervals until the distribution was unchanged, indicating that equilibrium had been reached. All plots shown represent equilibrium and span the length of the sample. Data sets at two or three rotor speeds were fit simultaneously with the program Current XLA, developed by Dr. D. McCaslin, University of Wisconsin–Madison Biophysics Instrumentation Facility. The plots shown represent single data sets.

Mass Spectroscopy. Peptides were analyzed with a Bruker Reflex II MALDI-TOF mass spectrometer. Data were collected with α-cyano-4-hydroxycinnamic acid matrix. Masses of HPLC-purified peptides are as follows (calculated mass; observed mass): **1** (4306.0; 4328.3), PyrGG-**1** (4691.1; 4688.8), FluGG-**1** (4895.5; 4895.1), DecGG-**1** (4823.6; 4823.1), HcGG-**1** (4769.4; 4768.7), PyrGG-**2** (3324.8; 3324.4), **3** (3630.0; 3629.8), PyrGG-**3** (3860.4; 3861.1), PyrGG-**4** (3860.4; 3859.7), **5** (2760.2; 2760.4), FluGG-**5** (3076.3; 3075.9), DecGG-**5** (3004.4; 3005.5), HcGG-**5** (2948.2; 2948.5), **6**, (4583.5; 4581.5), **7** (3829.1; 3827.9), and **8** (2998.8; 2997.6). The experimental mass for **1** corresponds to the addition of sodium (M + Na).

(23) Brandts, J. F.; Kaplan, L. J. *Biochemistry* **1973**, *12*, 2011–2024.

Amino Acid Analysis. Peptides were analyzed with a Perkin-Elmer-Applied Biosystems Model 421 Amino Acid Analyzer System. Conversion of peptides to free amino acids was carried out by hydrolysis at 165 °C for 1 h with vapor phase 6 N HCl. Norleucine was added prior to hydrolysis as an internal standard. The hydrolysate was dissolved in 0.25 mg/mL postassium EDTA. The solution was loaded onto the slide frits of the analyzer. Free amino acids were allowed to react with phenylisothiocyanate (PITC) to form phenylthiocarbamyl derivatives (PTC-AA). The derivatives were extracted and transferred to an on-line HPLC for analysis. The system uses an ABI Model 172 microbore HPLC equipped with a 220 × 2.1 mm PTC C-18 Brownlee column and an ABI Model 900A Data Analysis Module. Identity of the PTC-AAs was established by retention time. Quantification was based on peak height (detection at 254 nm). Calibration was achieved by parallel analysis of a standard amino acid mixture (Pierce, Rock Island, IL). Results were normalized to the measured recovery of norleucine.

Supporting Information Available: HPLC, sedimentation, CD, and fluorescence data for synthetic peptides. This material is available free of charge via the Internet at http://pubs.acs.org.

JA990178P